

# Use of site-directed mutagenesis to probe the structure, function and isoniazid activation of the catalase/oxidase, KatG, from *Mycobacterium tuberculosis*

Brigitte SAINT-JOANIS\*, H el ene SOUCHON†, Martin WILMING‡, Kai JOHNSSON‡, Pedro M. ALZARI† and Stewart T. COLE\*<sup>1</sup>

\*Unit  de G n tique Mol culaire Bact rienne, Institut Pasteur, 28 rue du Docteur Roux, 75724 Paris Cedex 15, France, †Unit  de Biochimie Structurale, Institut Pasteur, 28 rue du Docteur Roux, 75724 Paris Cedex 15, France, and ‡Lehrstuhl f r Organische Chemie I, Ruhr-Universit t Bochum, 44780 Bochum, Germany

A series of mutants bearing single amino acid substitutions often encountered in the catalase/oxidase, KatG, from isoniazid-resistant isolates of *Mycobacterium tuberculosis* has been produced by site-directed mutagenesis. The resultant enzymes were overexpressed, purified and characterized. Replacing Cys-20 by Ser abolished disulphide-bridge formation, but did not affect either dimerization of the enzyme or catalysis. The substitution of Thr-275, which is probably involved in electron transfer from the haem, by proline resulted in a highly unstable enzyme with insignificant enzyme activities. The most commonly occurring substitution in drug-resistant clinical isolates is the replacement

of Ser-315 by Thr; this lowered catalase and oxidase activities by 50% and caused a significant decrease in the KatG-mediated inhibition of the activity of the NADH-dependent enoyl-[acyl-carrier protein] reductase, InhA, *in vitro*. The ability of this enzyme to produce free radicals from isoniazid was severely impaired, as judged by its loss of NitroBlue Tetrazolium reduction activity. Replacement of Leu-587 by Pro resulted in marked instability of KatG, indicating that the C-terminal domain is also important for structural and functional integrity.

Key words: free radicals, mycolic acids, prodrugs.

## INTRODUCTION

In recent years, the mechanism of action of isoniazid (isonicotinic acid hydrazide; INH), a key anti-tuberculosis agent, has been the subject of intense study. It is now widely accepted that INH is a prodrug [1,2], which is converted into the active form by the haem-containing enzyme catalase/oxidase, encoded by the *katG* gene of *Mycobacterium tuberculosis* [3–5]. The precise nature of the active species is unknown, but it is clear that the stable products of the enzymic reaction, i.e. isonicotinic acid, isonicotinamide and pyridine-4-carboxaldehyde [1,2], are not toxic for tubercle bacilli at physiological concentrations. Instead, toxicity may be mediated *in vivo* by radicals that are capable of reacting with other cellular components.

One of the more obvious consequences of INH treatment is the inhibition of mycolic acid synthesis, leading to cell death [6]. Two enzyme systems that may intervene in mycolic acid production have been characterized extensively: the NADH-dependent enoyl-[acyl-carrier protein (ACP)] reductase, InhA [7–9], and the 3-oxoacyl ACP synthase, KasA [10], which are encoded by the genes *inhA* and *kasA* respectively. INH has been shown to inhibit the catalytic activity of InhA *in vitro* [2,8], and the co-crystal structure revealed the presence of isonicotinic acyl-NADH within the active site of InhA [11]. Likewise, radiolabelled INH was shown to be associated with a complex of the KasA protein and its ACP, AcpM, in *M. tuberculosis*, and biophysical examination suggested that the acyl-pyridine moiety of INH was bound to AcpM [10].

Mutations have been described in patient isolates of *M. tuberculosis* that lead to overexpression of *inhA* [12–15] or result

in amino acid substitutions in the InhA protein [9,11], and these are believed to be associated with low-level resistance to INH that is of limited clinical significance [12,16]. Recently, missense mutations have also been found in the *kasA* gene from INH-resistant strains, but direct evidence to account for drug resistance has not yet been obtained [10]. The principal mechanism of INH resistance is unquestionably mutation of *katG* [12–14,17,18], leading to abolition or reduction of catalase/oxidase activity [14,17–20]. This, in turn, results in lack of INH activation.

Some mutant alleles of *katG*, encoding enzymes with amino acid substitutions, are encountered more frequently than others in clinical isolates, and the corresponding strains often display differences in levels of KatG activity and INH resistance. One of the most intriguing mutations, affecting the active site, is the substitution of Ser-315 by threonine; although this lowers enzyme activity significantly, the INH resistance seems discrepantly high. In the present study, site-directed mutagenesis has been used to introduce this and other mutations into the cloned gene, and the corresponding enzyme variants have been purified and characterized biochemically in an attempt to gain further insight into the mechanism of activation of INH.

## EXPERIMENTAL

### Site-directed mutagenesis

Mutants of *katG* were obtained by using the Chameleon double-stranded site-directed mutagenesis kit (Stratagene) applied to the plasmid pKATII, an *Escherichia coli* expression vector containing the *katG* gene placed downstream of the tryptophan promoter [21]. The different primers used to achieve the mutagenesis are

Abbreviations used: INH, isonicotinic acid hydrazide (isoniazid); ACP, acyl-carrier protein; NBT, NitroBlue Tetrazolium; CCP, cytochrome c peroxidase.

<sup>1</sup> To whom correspondence should be addressed (e-mail [stcole@pasteur.fr](mailto:stcole@pasteur.fr)).

**Table 1 Primers used for mutagenesis**

The mutated nucleotide is shown in **bold**.

Primer location	Mutation	Mutagenic primer
<i>katG</i>	Cys-20 → Ser	5' C ACG GGA <b>GAG</b> CCG TTG CTA GC 3'
<i>katG</i>	Thr-275 → Pro	5' CC GGC GCC ATG <b>GGG</b> CTT ACC GAA AG 3'
<i>katG</i>	Ser-315 → Thr	5' GAC CTC GAT GCC <b>GGT</b> GGT GAT CGC G 3'
<i>katG</i>	Leu-587 → Met	5' G CCT TGG GCT CCA <b>TCA</b> CGG CAA AGG 3'
<i>katG</i>	Leu-587 → Pro	5' GCC TTG GGC TCC <b>GGC</b> ACG GCA AAG G 3'

described in Table 1. The desired nucleotide substitution in the genes encoding the mutant proteins was confirmed by dideoxynucleotide sequencing of the complete gene.

### Purification of the catalase/peroxidase KatG

*E. coli* UM262 (*recA katG::Tn10 pro leu rpsL hsdM hsdR end lac Y*) pKATII was grown in M9-glucose medium, supplemented with 50 mg/l  $\text{Fe}(\text{NH}_4)_2(\text{SO}_4)_2$  and 1 mg/l thiamin. Antibiotics were added at the following concentrations: ampicillin, 50  $\mu\text{g}/\text{ml}$ ; tetracyclin, 12.5  $\mu\text{g}/\text{ml}$ . Bacteria were grown in 0.5-litre culture at 37 °C, and expression was induced at an  $A_{600}$  of 0.8 by the addition of  $\beta$ -indolylacrylic acid (40 mg/l). Cells were grown for 16 h after induction, collected by centrifugation and then lysed by treatment with lysozyme, deoxycholic acid and DNase I in the presence of Pefablock (1 mM). The entire purification process was performed at 4 °C. Solid ammonium sulphate was added to the cell lysate to 10% saturation. After 30 min, the solution was centrifuged (15000 *g* for 30 min). The supernatant was collected and ammonium sulphate was added to 67% saturation. The precipitated proteins were collected by centrifugation; the pellet was dissolved in approx. 10 ml of buffer A (20 mM Bis-Tris/HCl, pH 6.9) and desalted on a PD10 column equilibrated with the same buffer. Eluted fractions, containing KatG activity, were pooled and applied directly to an anion-exchange column (Hi-Trap Q; 5 ml). The adsorbed protein was eluted with a 200 ml gradient from 0 to 0.5 M NaCl at a flow rate of 5 ml/min. Fractions containing KatG eluted between 0.20 and 0.25 M NaCl. The pooled eluted protein was concentrated by the addition of ammonium sulphate to 70% saturation. After 30 min, the precipitated protein was collected by centrifugation (15000 *g* for 30 min). The protein pellet was dissolved in buffer B (20 mM Bis-Tris/HCl, pH 6.9, 200 mM NaCl) and desalted on a PD10 column equilibrated with the same buffer. The eluted active fraction was concentrated on an Ultrafree-4 centrifugal filter unit (exclusion size 50 kDa). The concentrated fraction was loaded on to a gel-filtration column (Hi-Load 26/60 Superdex 200) equilibrated with buffer B and eluted at a linear flow rate of 1 ml/min. KatG was recovered in a homogeneous elution peak. The fraction collected was concentrated on Ultrafree centrifugal filter units. The final sample was frozen at -20 °C in small aliquots at a concentration of approx. 10 mg/ml. No decrease in activity was observed if the samples were thawed only once.

### Purification of KatG mutants

The process was identical to the one described above. However, in the case of an inactive mutant enzyme, the chromatographic fractions were screened by dot-blot using a polyclonal antibody directed against KatG [22].

### Enzyme assays

Catalase activity was determined spectrophotometrically by measuring the decrease in  $\text{H}_2\text{O}_2$  concentration at 240 nm ( $\epsilon_{240} = 0.0435 \text{ mM}^{-1} \cdot \text{cm}^{-1}$ ), at 25 °C. The reaction mixture (1 ml) contained 50 mM sodium phosphate buffer, pH 7.0, and 10 mM  $\text{H}_2\text{O}_2$ . Peroxidase activity was determined spectrophotometrically by measuring the rate of oxidation of 0.1 mM *O*-dianisidine at 460 nm ( $\epsilon_{460} = 11.3 \text{ mM}^{-1} \cdot \text{cm}^{-1}$ ) at 25 °C, in the presence of 23 mM *t*-butyl hydroperoxide in 50 mM sodium acetate buffer, pH 5.5 [23]. Specific activities were expressed as enzyme units/mg of total protein. The protein concentration was determined by the Bradford method [24].

### Activity gels

Catalase and peroxidase activities were also detected in native polyacrylamide gels using the process described previously [25].

### INH oxidation

The enzymic oxidation of INH by wild-type KatG or by the S315T mutant of KatG was performed in 50 mM  $\text{Na}_2\text{HPO}_4$ , pH 7.5, at 37 °C. The INH and KatG concentrations were 100  $\mu\text{M}$  and 1  $\mu\text{M}$  respectively. In the absence of  $\text{MnCl}_2$ , there was no background of auto-oxidation of INH, whereas in other experiments (results not shown) performed in the presence of 0.1  $\mu\text{M}$   $\text{MnCl}_2$ , auto-oxidation of INH was observed. Reaction aliquots were removed at defined times and quenched with a solution of 0.13 M  $\text{NH}_2\text{OH}$ , pH 6.8, containing 3-nitrobenzyl alcohol as an external standard. Samples were analysed on a reverse-phase nucleosil 100-5 C18AB column (Macherey and Nagel CC250/4) using a linear gradient prepared from 50 mM sodium acetate, pH 7.0, and acetonitrile. Concentrations of INH and isonicotinic acid were determined by integration of the HPLC profile monitored at 260 nm and comparison with the peak of 3-nitrobenzyl alcohol [1].

### Inactivation of InhA

Inactivation of His-tagged InhA in the presence of wild-type KatG and the S315T mutant of KatG was studied in 100 mM  $\text{Na}_2\text{HPO}_4$ , pH 7.5, 5  $\mu\text{M}$   $\text{MnCl}_2$ , 100  $\mu\text{M}$  INH and 70  $\mu\text{M}$   $\text{NAD}^+$  at 25 °C [2]. InhA and KatG concentrations were 4  $\mu\text{M}$  and 1.2  $\mu\text{M}$  respectively. A higher  $\text{MnCl}_2$  concentration was required as a result of the histidine tag on InhA. Reaction aliquots were removed at defined times and analysed for InhA activity utilizing the substrate 2-*trans*-octenoyl-CoA (625  $\mu\text{M}$ ) and NADH (130  $\mu\text{M}$ ). Rates were determined by following the decrease in the concentration of NADH at  $A_{340}$ .

### Reduction of NitroBlue Tetrazolium (NBT)

Reduction was monitored qualitatively following electrophoresis of catalase/peroxidase on native gels [26]. The gel was soaked in 50 ml of 50 mM sodium phosphate, pH 7.0, containing 68 mg of INH, 12.5 mg of NBT and 15  $\mu\text{l}$  of 30%  $\text{H}_2\text{O}_2$ . Colour development was complete after 30 min; the gel was then rinsed with distilled water and soaked in 7% acetic acid/1% glycerol before photographs were taken. For quantitative purposes, a spectrophotometric assay was employed at 25 °C. The reaction mixture consisted of 0.2 mM NBT in 50 mM sodium phosphate buffer (pH 7.0) to which INH (7.5 mM) and about 1  $\mu\text{g}$  of enzyme (wild-type KatG or mutant enzymes) were added. The

reactions were initiated by the addition of H<sub>2</sub>O<sub>2</sub> (500 µM). Changes in A<sub>560</sub> were recorded during 10 min in a double-beam spectrophotometer.

## Materials

Pefablock SC was obtained from Interchim. PD10, Hi-Trap Q and Hi-Load 26/60 Superdex 200 columns were purchased from Pharmacia Biotech Inc. Ultrafree centrifugal filter units were obtained from Millipore. Polyclonal anti-KatG antiserum was made by immunizing a rabbit with purified wild-type KatG [22].

## RESULTS

### Rationale for site-directed mutagenesis

Bacterial catalase/peroxidases have evolved by gene duplication [27,28] and consist of three domains (Figure 1): a short segment of ~54 amino acid residues at the N-terminus containing a highly conserved cysteine (Cys-20 in *M. tuberculosis* KatG), followed by the catalytic domain (residues 55–423) carrying the active site and the haem-binding region of the enzyme, and finally the C-terminal domain (residues 424–740). The role of the final segment, which is highly related to the central catalytic domain, is obscure. Many INH-resistant strains of *M. tuberculosis* harbour missense mutations in *katG*; when these occur in the sequences encoding the catalytic domain the level of resistance is generally high, whereas most of the mutations affecting the C-terminal part are either associated with low-level resistance or appear to be without effect. One of the most commonly encountered amino acid substitutions is the replacement of Ser-315, which binds haem and is probably part of the ligand-access channel of the enzyme, by Thr [17,20]. This and several other independent mutations were introduced into *katG* by site-directed mutagenesis and incorporated into the pKATII vector. Among the other single amino acid substitutions chosen were C20S, T275P, L587M and L587P (Figure 1). This last mutation has been found in the highly resistant *M. bovis* strain WAg405 (N.

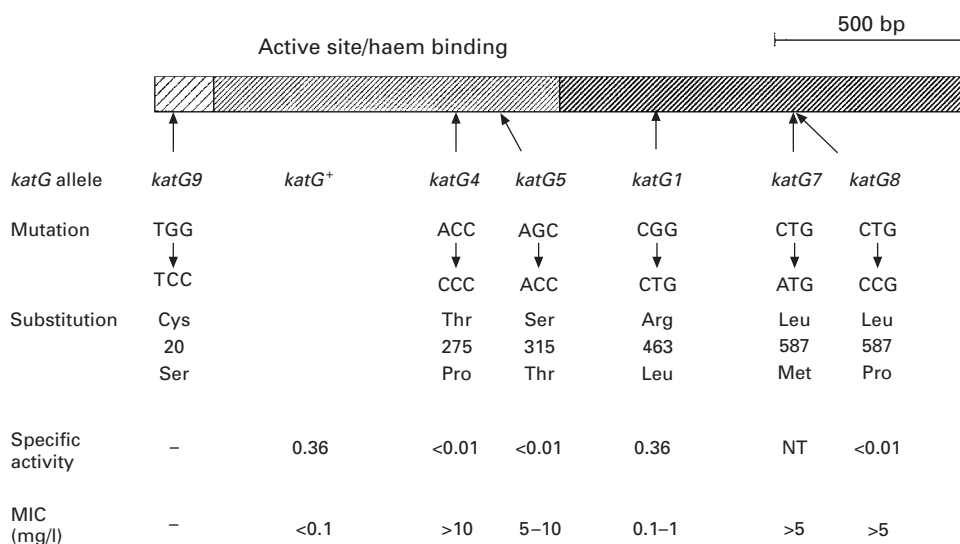
**Table 2** Purification of KatG

Step	Total protein (mg)	10 <sup>-3</sup> × Total catalase activity (units)	Specific catalase activity (units/mg)	Recovery (%)	Purification (fold)
Cellular lysate	275	28.8	104	100	1
(NH <sub>4</sub> ) <sub>2</sub> SO <sub>4</sub> precipitation	79	16.6	209	58	2
Anion-exchange Hi-Trap Q	16	13	826	45	7.9
Gel-filtration Superdex 200	10	10.4	1035	36	10

Honoré and S. T. Cole, unpublished work), which completely lacks catalase/peroxidase activity [29].

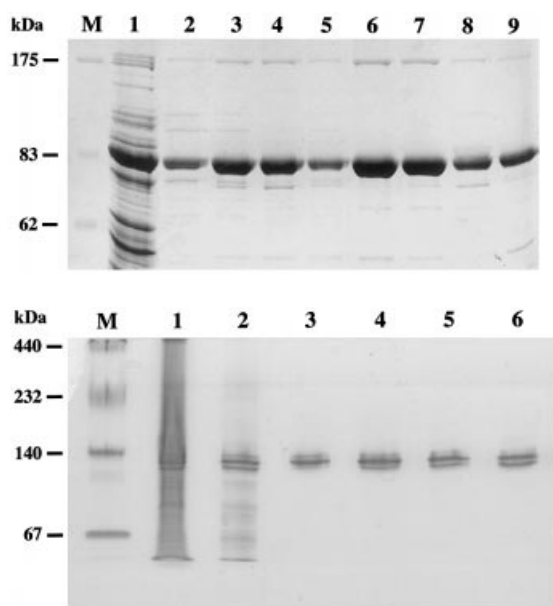
### Some biochemical properties of recombinant wild-type KatG

Table 2 presents typical results obtained with purified recombinant wild-type KatG. This protein appeared as a single band on SDS/polyacrylamide gels with an apparent molecular mass of 81 kDa (Figure 2, upper panel). The mass was estimated at 80494 atomic mass units by means of electrospray MS, indicating that the initiating formyl-methionine residue had been removed (as found by Edman degradation) and that no other post-translational covalent modifications had occurred. When analysed on non-denaturing PAGE, the recombinant protein migrated as a dimer with three isoforms (Figure 2, lower panel), the largest of which, a minor species lacking haem, is devoid of catalase and peroxidase activities. Partial separation of the two active bands can be obtained by including an additional high-resolution chromatographic step [21], and this suggested that the two forms of KatG differ in haem content, with RZ values ( $A_{406}/A_{280}$ ) of 0.4 and 0.7 respectively (results not shown). When analysed by



**Figure 1** Mutations of the *katG* gene of *M. tuberculosis*

The corresponding amino acid substitutions and the three-domain structure are shown. The minimal inhibitory concentration (MIC) values for INH were determined with *M. tuberculosis* strains carrying *katG*<sup>+</sup> or the mutant alleles, and the specific activities indicated (units/mg) were determined in crude extracts. NT, not tested.



**Figure 2** Purification of recombinant *M. tuberculosis* KatG

Upper panel: analysis on denaturing gels, stained with Coomassie Blue. Positions of molecular mass standards (Biolabs) are shown (lane M). Lane 1, crude extract; lanes 2–5, fractions eluted from the anion-exchange column (Hi-Trap Q); lanes 6–9, fractions eluted from the gel-filtration column (Hi-Load 26/60 Superdex 200). Lower panel: non-denaturing gel analysis. Positions of molecular mass standards (Pharmacia) are shown (lane M). Lane 1, crude extract; lane 2, peak fraction from the anion-exchange column (Hi-Trap Q); lanes 3–6, fractions eluted from the gel-filtration column (Hi-Load 26/60 Superdex 200).

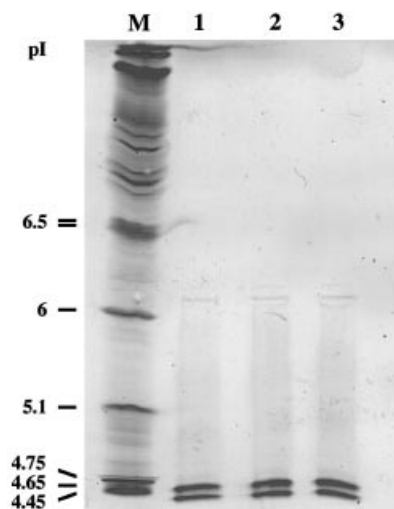


**Figure 3** Isoelectric focusing

Samples were subjected to isoelectric focusing on a gel of pI 3–9. Lane M contains broad-pI (3.5–9.3) calibration markers. Lanes 1–3 contain purified samples of wild-type KatG.

isoelectric focusing, the protein was also present as two species with pI values of 4.5 and 4.6 (Figure 3).

#### Purification of variant KatG proteins

The pKATII expression system was used to overproduce the other KatG variants, and these were purified from *E. coli* and

**Table 3** Catalase activity of KatG wild type (WT) and mutants

ND, not determined.

Enzyme	$k_{\text{cat}}$ ( $\text{s}^{-1}$ )	$V_{\text{max}}$ (% of WT)	$K_{\text{m}}$ (mM)	$10^6 \times k_{\text{cat}}/K_{\text{m}}$ ( $\text{M}^{-1} \cdot \text{s}^{-1}$ )
KatG WT	2830 ± 450	100	4 ± 1	0.7 ± 0.1
KatG C20S	2950 ± 440	104	6.6 ± 1.4	0.4 ± 0.1
KatG T275P	25 ± 5	1	ND	–
KatG S315T	1470 ± 200	52	5.5 ± 0.5	0.3 ± 0.1
KatG R463L	2635 ± 500	93	4.4 ± 1.6	0.6 ± 0.1
KatG L587M	2880 ± 500	102	7.2 ± 1.8	0.4 ± 0.1
KatG L587P	ND	–	ND	–

analysed in essentially the same manner. Four of the mutant KatG enzymes were expressed to high levels representing 2–4% of total cellular protein, whereas the variants KatG T275P and KatG L587P were found to be respectively difficult to overexpress and unstable. Reproducible yields of close to 20 mg/l were obtained with the wild-type, KatG C20S, KatG R463L and KatG L587M enzymes, but only half this amount was generated from UM262 overexpressing KatG S315T in several different experiments.

#### Kinetic characterization of variant KatG proteins

Wild-type recombinant KatG was characterized kinetically, and the apparent  $K_{\text{m}}$  and  $k_{\text{cat}}$  values were determined for the catalase and peroxidase reactions using  $\text{H}_2\text{O}_2$  and t-butyl hydroperoxide respectively. These kinetic parameters were found to be similar to those reported previously [21,30] and are presented in Tables 3 and 4, where they are compared with the corresponding values obtained with the other variants of KatG. Three of the enzymes (KatG C20S, KatG R463L and KatG L587M) behaved very similarly to the wild-type enzyme in these assays, while two variants displayed statistically significant differences. As the catalase activity of KatG T275P was reduced by 100-fold and its peroxidase activity was also considerably diminished, the  $K_{\text{m}}$  could not be determined. These activities were also decreased in the S315T variant, to about 50% of the wild-type level, although the  $K_{\text{m}}$  values for  $\text{H}_2\text{O}_2$  and t-butyl hydroperoxide were not significantly affected (Tables 3 and 4).

The haem content of both the KatG T275P and S315T proteins was lower than that observed for the other enzymes (RZ values of 0.1 and 0.3, compared with > 0.5 for wild-type KatG), and when the S315T enzyme was examined on activity gels the relative abundance of the third, haem-free, isoform was found to have increased significantly (results not shown).

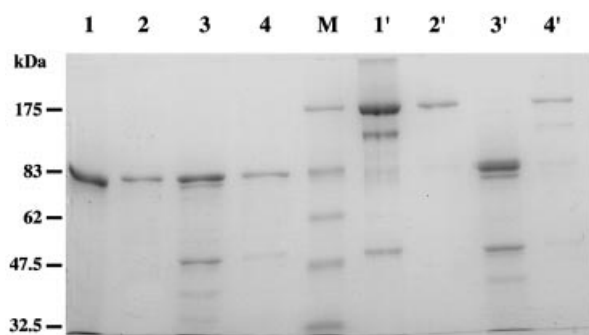
#### Disulphide-bridge formation

A single cysteine residue is conserved among all the catalase/peroxidases of the KatG family, and this suggested that formation of a disulphide bridge could be involved in dimerization or subunit–subunit interactions. When the C20S variant of KatG was analysed by means of electrophoresis on SDS/polyacrylamide gels under reducing and non-reducing conditions, a major species of molecular mass 81 kDa was seen in both cases (Figure 4). By contrast, all of the other KatG variants displayed prominent bands of molecular mass 160 kDa under non-reducing conditions that disappeared when dithiothreitol was present. These results indicate that KatG is a dimeric enzyme with a single disulphide bond formed by the thiol groups of Cys-20 in

**Table 4** Peroxidase activity of KatG wild type (WT) and mutants

ND, not determined.

Enzyme	$k_{\text{cat}}$ ( $\text{s}^{-1}$ )	$V_{\text{max}}$ (% of WT)	$K_m$ (mM)	$10^4 \times k_{\text{cat}}/K_m$ ( $\text{M}^{-1} \cdot \text{s}^{-1}$ )
KatG WT	$0.7 \pm 0.1$	100	$0.06 \pm 0.01$	$1.2 \pm 0.3$
KatG C20S	$0.8 \pm 0.1$	114	$0.06 \pm 0.03$	$1.3 \pm 0.3$
KatG T275P	$0.05 \pm 0.01$	7	ND	—
KatG S315T	$0.35 \pm 0.02$	50	$0.07 \pm 0.03$	$0.5 \pm 0.1$
KatG R463L	$0.7 \pm 0.1$	100	$0.08 \pm 0.02$	$0.9 \pm 0.3$
KatG L587M	$0.6 \pm 0.1$	86	$0.05 \pm 0.02$	$1.2 \pm 0.4$
KatG L587P	ND	—	ND	—

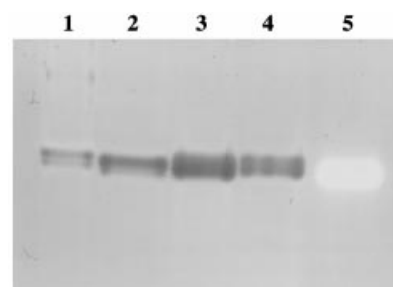
**Figure 4** Analysis of disulphide-bridge formation

Disulphide-bridge formation was analysed by SDS/PAGE under reducing or non-reducing conditions and Coomassie Blue staining. Positions of molecular mass standards (Biolabs) are shown (lane M). Lanes 1–4, samples of purified enzymes in loading buffer containing dithiothreitol (reducing conditions): 1, KatG; 2, KatG R463L; 3, KatG C20S; 4, KatG S315T. Lanes 1'–4', samples of purified enzymes in loading buffer without dithiothreitol (non-reducing conditions): 1', KatG; 2', KatG R463L; 3', KatG C20S; 4', KatG S315T.

each subunit. The C20S substitution abolished disulphide-bridge formation, but did not affect either dimerization, as indicated by gel-filtration chromatography, or catalase and peroxidase activities (Tables 3 and 4).

### Substitution of Leu-587

In one INH-resistant clinical isolate of *M. tuberculosis*, Leu-587 of KatG had been replaced by Met and the corresponding enzyme retained significant activity [20], whereas this position is occupied by Pro in WAg405, a laboratory mutant of *M. bovis* that is devoid of KatG activity. When the recombinant KatG L587M was characterized biochemically, no significant differences were observed in any of the enzymic parameters measured (Tables 3 and 4). By contrast, replacing Leu-587 by Pro resulted in the loss of all enzyme activities and marked instability of the protein (results not shown). Indeed, no full-sized KatG could be detected in *E. coli*, although a protein of molecular mass 57 kDa was found that could be immunoprecipitated by antibodies to KatG. To confirm that proteolysis of KatG L587P also occurred in the INH-resistant *M. bovis* strain, protein extracts of WAg405 were analysed by immunoblotting. Again, the only protein recognized by the polyclonal anti-KatG serum was of molecular mass 57 kDa, while the parental strain produced the full-size enzyme (results not shown).

**Figure 5** NBT reduction activity gel

Lanes 1–5 contain approx.  $1 \mu\text{g}$  samples of purified enzymes: 1, KatG; 2, KatG R463L; 3, KatG C20S; 4, KatG L587M; 5, KatG S315T.

### Proteolysis of KatG

SDS/PAGE analysis also revealed partial degradation of the wild-type KatG protein, with two minor species of apparent molecular masses of 54 and 45 kDa. The N-terminal residues of these truncated proteins were determined and found to correspond to Ala-256 and Asp-311 respectively, indicating that the cleavage sites occur in two loops close to the active site of the first peroxidase-like domain of KatG. Interestingly, the C20S variant form of KatG appeared to be more prone to degradation (Figure 4), suggesting that the disulphide bond may stabilize the protein. In contrast, SDS/PAGE and MS of the S315T mutant enzyme did not reveal internal proteolysis.

### Further characterization of KatG S315T

To determine whether the S315T variant generated the same reaction products as the wild-type enzyme, a series of additional measurements was performed. The two enzymes were incubated independently with INH and the rate of formation of isonicotinic acid, the final product of the reaction, was measured. The KatG S315T protein produced  $0.11 \pm 0.01 \mu\text{mol}/\text{min}$ , representing roughly 5-fold lower activity than that of the wild-type enzyme ( $0.51 \pm 0.08 \mu\text{mol}/\text{min}$ ). Its ability to inactivate the InhA protein in the presence of INH was also studied, and this was found to be greatly decreased compared with the wild-type enzyme. The percentage inactivation of InhA mediated by wild-type KatG was  $69 \pm 18\%$  after 60 min of incubation, whereas the level of inactivation of InhA mediated by the S315T variant ( $22 \pm 3\%$ ) was not significantly different from that resulting from auto-oxidation of INH ( $21 \pm 13\%$ ).

### INH-dependent reduction of NBT

The KatG enzyme is known to produce radical species [1,31], and these can be detected by means of the NBT reduction assay [26]. Initially this was monitored on activity gels, where it was found that, unlike all the other enzymes tested, the S315T variant was unable to reduce NBT to formazan when INH was present (Figure 5). To quantify this activity, a spectrophotometric assay was devised; under these conditions, the KatG S315T enzyme ( $0.001 \pm 0.0005$  unit/mg of protein) was found to show  $> 90\%$  lower activity than the wild-type protein and the variants KatG C20S, KatG R463L and KatG L587M ( $0.01 \pm 0.001$  unit/

mg). Interestingly, when INH was replaced in this assay by nicotinic acid hydrazide, no reduction of NBT occurred.

## DISCUSSION

The aim of this study was to use site-directed mutagenesis to produce some of the commonly occurring *katG* alleles present in INH-resistant clinical isolates of *M. tuberculosis*, and then to overexpress and purify the corresponding enzymes in an attempt to elucidate the biochemical basis of activation of INH by catalase/peroxidase and to understand the mechanism of resistance. Our initial efforts concentrated on two residues that were predicted to be important components of the active site [20] (Thr-275 and Ser-315), two residues in the C-terminal domain (Arg-463 and Leu587), and the sole cysteine residue (Cys-20), which is conserved in all bacterial catalase/peroxidases of the KatG type.

Replacement of Cys-20 by Ser abolished the formation of the single disulphide bridge, but did not affect dimerization of KatG or any of the catalytic activities measured, suggesting that the disulphide bond probably plays a minor structural role that is of no significance for drug resistance. One of the substitutions in the C-terminal domain of KatG, R463L, left enzyme activity unaffected, and this form of the enzyme is now believed to be a naturally occurring variant that is not associated with clinical INH resistance [19,21]. When the recombinant KatG L587M was characterized biochemically, no significant differences were observed in any of the enzymic parameters measured (Tables 3 and 4), suggesting that the INH resistance observed in the original study [20] may have been due to another mechanism. However, the replacement L587P, a mutation that has been described in KatG from INH-resistant *M. bovis*, resulted in marked instability of the enzyme. When expressed in either *M. bovis* or *E. coli*, the L587P variant underwent rapid and quantitative proteolysis. This finding is noteworthy, as it both demonstrates the significance of the C-terminal domain for stabilizing subunit-subunit interactions and highlights the importance for molecular diagnostic purposes of monitoring the whole *katG* gene for the presence of mutations [16].

Replacement of Ser-315 by Thr is by far the most abundant substitution encountered in strains of *M. tuberculosis* resistant to clinically significant levels of INH, and accounts for ~ 50% of the mutations found in our collection. Other workers have reported similar findings [17], and in some strains Ser-315 is replaced by Asn. Mutation of the Ser-315 codon to that for Thr has also been seen to occur during treatment in a strain from a non-compliant tuberculosis patient who relapsed with INH-resistant disease (M. Sofia, B. Heym, N. Honoré and S. T. Cole, unpublished work). These combined epidemiological observations testify to the importance of this amino acid residue in INH resistance, yet its replacement by Thr resulted in only 50% decreases in both catalase and peroxidase activities. This is curious, because *in vivo* the S315T substitution is accompanied by a greater than 50-fold increase in the minimal inhibitory concentration for INH that is difficult to explain solely on the basis of the lowered enzyme activities of the purified KatG variant.

Two possible explanations spring to mind: alterations in enzyme stability or differences in the rate of generation of reaction products. It is conceivable that the S315T substitution renders the enzyme less stable in the bacterium, resulting in lower levels of activation of INH and concomitant drug resistance. In an earlier study [20], this enzyme was found to be rather more heat labile in crude extracts than the wild-type enzyme, although other workers found no significant difference in the amount of

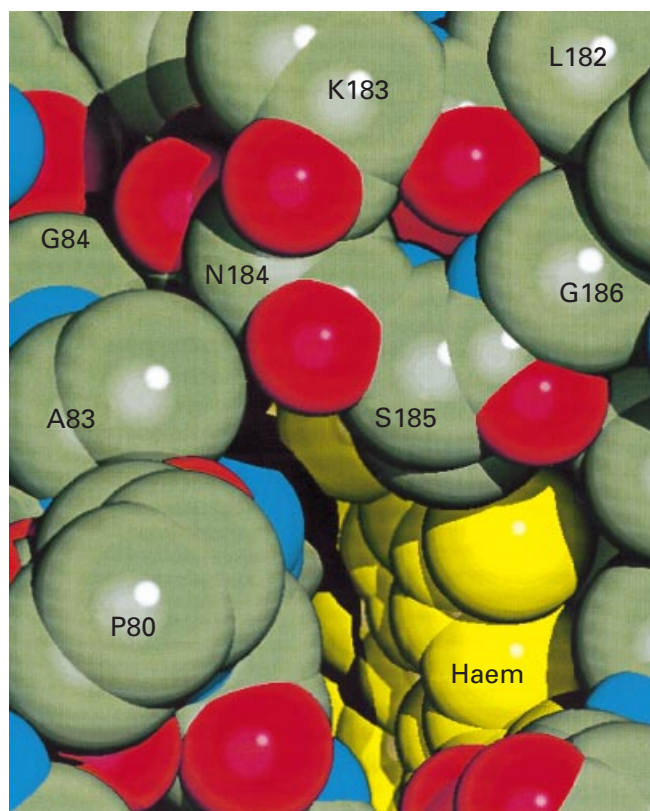


**Figure 6** Space-filling model of the active site of CCP

The co-ordinates for the yeast enzyme were obtained from PDB (entry code 1ccp [32]), and the model shows the substrate-access channel. The haem group is shown in yellow, and the amino acid residues discussed in the text are labelled (one-letter code).

protein produced in cells, as determined by immunoblotting [19]. Comparison of the thermal stability of the wild-type and S315T enzymes revealed no significant difference (results not shown).

While our work was in progress, Wengenack et al. [30] reported the findings of a similar study with purified recombinant KatG S315T, which essentially agree with those presented here. These workers found that the wild-type enzyme was more efficient than the mutant form at converting INH into isonicotinic acid, but that this was more pronounced at higher drug concentrations which may not be encountered physiologically. This effect has been confirmed here at a lower concentration. It is also shown that a striking difference between the two enzymes occurs in their ability to reduce NBT, an assay that measures free-radical production, and this is accompanied by a marked decrease in the inhibition of InhA activity. Most significantly, reduction of NBT did not occur when INH was replaced by nicotinic acid hydrazide, despite its oxidation to nicotinic acid [1]. Presumably, acyl radical formation may be mediated in a stereospecific manner by the active site of KatG.

In the absence of an experimental three-dimensional model of bacterial catalase/peroxidases, the crystallographic model [32] of the highly similar cytochrome *c* peroxidase (CCP) can provide some structural insight into the effects of the S315T substitution. In this structure, the hydroxy group of the equivalent serine residue (Ser-185) forms a strong hydrogen bond with the 'outer' propionate carboxylate of the haem group (Figure 6), suggesting that partial disruption of this interaction would result in a

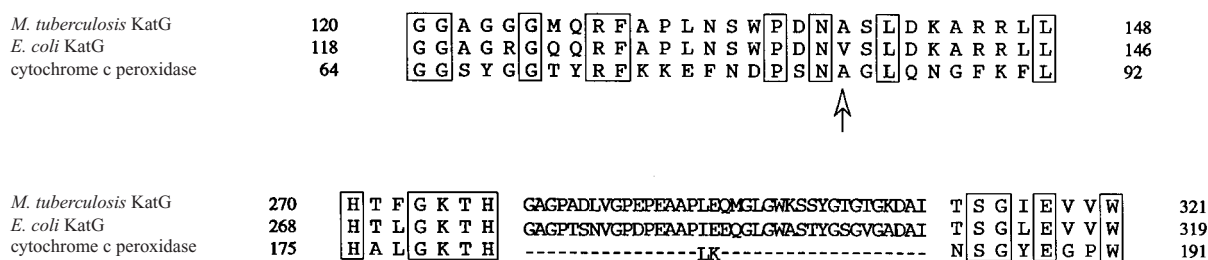


**Figure 7** Amino acid sequence alignment of active-site regions corresponding to labelled residues in Figure 6

The alignment shows amino acid residues present in two loops close to the active sites of catalase/peroxidases from *M. tuberculosis* and *E. coli*, together with the paradigm for this family, CCP from yeast. Residues conserved in all three enzymes are boxed. The arrow indicates the position of Val-137 in the *E. coli* enzyme discussed in the text.

protein variant with a lower haem content ([30]; the present study).

All bacterial catalase/peroxidases have, with respect to CCP [32], a 35-amino-acid insertion in the Ser-315-containing loop (Figure 7), which has been suggested to play a role in the constitution of the ligand-access channel to the active site of the enzyme [20]. Close inspection of the three-dimensional structure and sequence alignment in this region suggests that Ser-315 in mycobacterial KatG (Ser-313 in *E. coli*) should play a similar structural role to Ser-185 in CCP, with the bacterial insertion most probably occurring at the tip of the CCP loop, around positions 182–184 (Figure 7). It would then follow that the substitution of a serine residue by threonine will introduce an additional methyl group, interfering directly with the substrate-binding site and/or access channel (Figure 6). This is expected to introduce steric constraints in the active site for certain substrates such as INH. A similar effect is predicted for the less frequently observed S315N substitution.

This structural hypothesis is consistent with the significant changes in the catalytic constants for INH observed between wild-type and S315T KatG by Wengenack et al. [30]. These authors found that wild-type KatG has  $k_{cat}$  and  $K_m$  values that are 7- and 5-fold higher respectively than those observed for the S315T mutant. The CCP structure shows that the substrate-access channel is also limited by a second loop, which has the same length in CCP and KatG (Figure 7). In the CCP structure, two amino acid residues from this loop, Ala-83 and Gly-84, are directly facing the loop containing Ser-185, suggesting that the substitution of Ala-83 by a residue with a bulkier side chain could also interfere with substrate access to the active site (and therefore modify the enzymic properties of the enzyme). In *M. tuberculosis* KatG, an alanine residue (Ala-139) occupies the position equivalent to Ala-83 in CCP, whereas a bulkier valine side chain is found at the same position in *E. coli* KatG (Figures 6 and 7). It is tempting to speculate that the Ala → Val substitution in the *E. coli* enzyme might produce a similar effect to the S315T substitution in *M. tuberculosis* KatG (i.e. adding methyl groups that interfere with substrate binding). This could explain why, under conditions of constant peroxide flux, Hillar and Loewen [26] found a significantly lower rate of radical generation from INH by the *E. coli* enzyme compared with recombinant *M. tuberculosis* KatG, despite their very similar peroxidase activities. It is interesting to note that, in catalase A from yeast, the substitution of a valine residue by alanine, thought to relieve steric constraints in the major substrate channel but not directly affecting the active site, significantly altered the catalytic properties of the enzyme, decreasing the catalase activity and markedly increasing the peroxidase activity [33].

Another interesting property of KatG S315T is the decreased level of proteolytic cleavage observed. As outlined above, proteolysis occurred to a minor extent in the two loops flanking the active site of all enzymically active KatG derivatives, and has also been seen with preparations of the wild-type *E. coli* enzyme (P. M. Alzari and I. Fita, unpublished work). In contrast, SDS/PAGE and MS of the S315T mutant enzyme did not reveal internal proteolysis of the protein, thus raising the intriguing possibility of self-proteolysis in wild-type KatG. Rapid degradation of the T275P variant of KatG probably explains the difficulties encountered in working with this form of the enzyme [19,20].

KatG is an important virulence factor in the pathogenesis of tuberculosis, as illustrated by the remarkable attenuation of the *M. bovis* mutant WAg405 (KatG L587P) in guinea pigs [29] and by other studies with *katG* mutants [22]. As suggested by the epidemiological analysis, it is likely that *M. tuberculosis* strains producing KatG S315T have a selective advantage *in vivo*, as they are resistant to clinically significant levels of INH, and since their catalase/peroxidase activities are not significantly impaired they should be more able to withstand the reactive oxygen species produced by the macrophage. This hypothesis should now be tested with strains bearing defined *katG* lesions.

We thank Octavian Barzû and Abdelkader Namane for performing MS, and Bill Jacobs, Robert Sarfaty, Catherine Guerreiro-Inverno, Des Collins and Theresa Wilson for supplying materials, reagents and technical support. This work received financial support from the BIOMED programme of the European Community (BMH4-CT97-2277), the Association Française Raoul Follereau, and the Institut Pasteur.

## REFERENCES

- 1 Johnsson, K. and Schultz, P. G. (1994) *J. Am. Chem. Soc.* **116**, 7425–7426
- 2 Johnsson, K., King, D. S. and Schultz, P. G. (1995) *J. Am. Chem. Soc.* **117**, 5009–5010
- 3 Heym, B., Zhang, Y., Poulet, S., Young, D. and Cole, S. T. (1993) *J. Bacteriol.* **175**, 4255–4259
- 4 Zhang, Y., Heym, B., Allen, B., Young, D. and Cole, S. (1992) *Nature (London)* **358**, 591–593
- 5 Zhang, Y., Garbe, T. and Young, D. (1993) *Mol. Microbiol.* **8**, 521–524
- 6 Winder, F. G. (1982) in *The Biology of the Mycobacteria* (Ratledge, C. and Stanford, J., eds.), pp. 353–438, Academic Press, New York
- 7 Dessen, A., Quémard, A., Blanchard, J. S., Jacobs, Jr., W. R. and Sacchettini, J. C. (1995) *Science* **267**, 1638–1641
- 8 Quémard, A., Sacchettini, J. C., Dessen, A., Vilcheze, C., Bittman, R., Jacobs, W. J. and Blanchard, J. S. (1995) *Biochemistry* **34**, 8235–8241
- 9 Banerjee, A., Dubnau, E., Quémard, A., Balasubramanian, V., Um, K. S., Wilson, T., Collins, D., de Lisle, G. and Jacobs, Jr., W. R. (1994) *Science* **263**, 227–230
- 10 Mdluli, K., Slayden, R. A., Zhu, Y.-Q., Ramaswamy, S., Pan, X., Mead, D., Crane, D. D., Musser, J. M. and Barry, III, C. E. (1998) *Science* **280**, 1607–1610

- 11 Rozwarski, D. A., Grant, G. A., Barton, D. H. R., Jacobs, Jr., W. R. and Sacchetini, J. C. (1998) *Science* **279**, 98–102
- 12 Heym, B., Honoré, N., Truffot-Pernot, C., Banerjee, A., Schurra, C., Jacobs, Jr., W. R., van Embden, J. D. A., Grosset, J. H. and Cole, S. T. (1994) *Lancet* **344**, 293–298
- 13 Heym, B. and Cole, S. T. (1997) *Int. J. Antimicrob. Agents* **8**, 61–70
- 14 Musser, J. M. (1995) *Clin. Microbiol. Rev.* **8**, 496–514
- 15 Mdluli, K., Sherman, D. R., Hickey, M. J., Kreiswirth, B. N., Morris, S., Stover, C. K. and Barry, III, C. E. (1996) *J. Infect. Dis.* **174**, 1085–1090
- 16 Telenti, A., Honoré, N., Bernasconi, C., March, J., Ortega, A., Heym, B., Takiff, H. E. and Cole, S. T. (1997) *J. Clin. Microbiol.* **35**, 719–723
- 17 Musser, J. M., Kapur, V., Williams, D. L., Kreiswirth, B. N., van Soolingen, D. and van Embden, J. D. (1996) *J. Infect. Dis.* **173**, 196–202
- 18 Rouse, D. A., Li, Z., Bai, G.-H. and Morris, S. L. (1995) *Antimicrob. Agents Chemother.* **39**, 2472–2477
- 19 Rouse, D. A., deVito, J. A., Li, Z., Byer, H. and Morris, S. L. (1996) *Mol. Microbiol.* **22**, 583–592
- 20 Heym, B., Alzari, P., Honoré, N. and Cole, S. T. (1995) *Mol. Microbiol.* **15**, 235–245
- 21 Johnsson, K., Froland, W. A. and Schultz, P. G. (1997) *J. Biol. Chem.* **272**, 2834–2840
- 22 Heym, B., Stavropoulos, A., Domenech, P., Honoré, N., Saint-Joanis, B., Wilson, T. M., Collins, D. M., Colston, M. J. and Cole, S. T. (1997) *Infect. Immun.* **65**, 1395–1401
- 23 Marcinkeviciene, J. A., Magliozzo, R. S. and Blanchard, J. S. (1995) *J. Biol. Chem.* **270**, 22290–22295
- 24 Bradford, M. M. (1976) *Anal. Biochem.* **72**, 248–254
- 25 Heym, B. and Cole, S. T. (1992) *Res. Microbiol.* **143**, 721–730
- 26 Hillar, A. and Loewen, P. C. (1995) *Arch. Biochem. Biophys.* **323**, 438–446
- 27 Welinder, K. G. (1991) *Biochim. Biophys. Acta* **1080**, 215–220
- 28 Welinder, K. G. (1992) *Curr. Opin. Struct. Biol.* **2**, 388–393
- 29 Wilson, T. M., de Lisle, G. W. and Collins, D. M. (1995) *Mol. Microbiol.* **15**, 1009–1115
- 30 Wengenack, N. L., Uhl, J. R., St. Amand, A. L., Tomlinson, A. J., Benson, L. M., Naylor, S., Kline, B. C., Cockerill, III, F. R. and Rusnak, F. (1997) *J. Infect. Dis.* **176**, 722–727
- 31 Shoeb, H. A., Bowman, Jr., B. U., Ottolenghi, A. C. and Merola, A. J. (1985) *Antimicrob. Agents Chemother.* **27**, 404–407
- 32 Wang, J., Mauro, J. M., Edwards, S. L., Oatley, S. J., Fishel, L. A., Ashford, V. A., Xuong, N. H. and Kraut, J. (1990) *Biochemistry* **29**, 7160–7173
- 33 Zamocky, M., Herzog, C., Nykyri, L. M. and Koller, F. (1995) *FEBS Lett.* **367**, 241–245

Received 29 September 1998/6 November 1998; accepted 16 December 1998